The Astrophysical Journal, 647:564–572, 2006 August 10

PULSATING SPECTRUM OF SUBDWARF STAR PG 1605+072: COMPARATIVE TIME-FREQUENCY ANALYSIS VIA WAVELET PACKET AND LOCAL SINE PACKET TRANSFORMS OF AN INTERRUPTED LIGHT CURVE

Pedro Jorge,[1] Amaro Rica da Silva,[2] and Ilídio Lopes[2,3,4]
Received 2005 November 1; accepted 2006 March 17

ABSTRACT

We present the time-frequency analysis of an interrupted light-curve time series of the pulsating subdwarf B (sdB) star PG 1605+072. From the data of a eight-night observational run we have determined the pulsating spectrum of PG 1605+072. We used both wavelet packet transform (WPTs) and localized sine packet transform (LSPTs) analysis to compare frequency determinations with previous results based on Fourier methods and their typical modeling of signals by strictly harmonic contributions. The procedures adopted here allow the determination of the pulsating spectrum of the combined night runs of data with a reduction of the usual alias peaks produced by the daytime observing gaps, thus providing a clean and compact spectrum. We also use various compression techniques to study signal reconstruction under WPT.

Subject headings: methods: data analysis — stars: individual (PG 1605+072) — stars: oscillations — subdwarfs

Online material: color figures

1. INTRODUCTION

The discovery of pulsations in subdwarf B (sdB) stars provides an excellent opportunity to probe sdB interiors using asteroseismological tools. While it is generally accepted that sdBs are similar to extreme horizontal branch stars, many questions remain unanswered regarding their formation and evolution. Of all the known pulsating stars, PG 1605+072 has the most extreme properties among sdB stars. This star is expected to have the richest spectrum of almost 50 modes, with the longest periods up to 550 s. In the past, PG 1605+072 has been observed many times either with photometry observations, measuring luminosity variations, or with spectroscopic observations measuring the redshift of emission lines (Koen et al. 1998; Kilkenny et al. 1999; O'Toole et al. 2002; Woolf et al. 2002; Falter et al. 2003; Pereira & Lopes 2004, 2005).

This paper is concerned with the comparative determination of a stellar pulsation spectrum of the star PG 1605+072 by two different time-frequency analyzing methods: the local sine packet transform (LSPT) and the wavelet packet transform (WPT). Our goal is to compare the estimates of the stellar power spectrum with those using conventional harmonic analysis as was made in Pereira & Lopes (2004). The technique seems to be quite successful in computing a power spectrum with reduced alias peaks produced by large intervals of daytime observational gaps. Previous attempts to use alternative techniques to Fourier analysis on the study of observational time series were made by Serre et al. (1995).

The study of observational time series, namely, photometric light curves and spectroscopic studies of velocity variations (Goupil et al. 1991; Vigouroux & Delache 1993), has long been used in stellar astronomy, although the systematic use of classical Fourier analysis in the study of poor signal-to-noise ratio data, as well as the inability to obtain uninterrupted time series of spectroscopic and photometric data, has recently emphasized the need for a more optimal approach to observational data reduction.

While Fourier techniques may be well suited for very long uninterrupted time series of periodic processes, deviations from harmonicity, noise, and irregular samplings introduce inevitable artifacts in the Fourier spectra. With Fourier analysis, the introduction of windowing to model observational data with night/day gaps causes a necessary loss in frequency resolution (for nonsquare windows) and the appearance of false bumps near a strong peak (for square windows). Gaussian windows are usually used as a good compromise.

A strong argument in support of wavelet analysis is the possibility of periodic nonharmonic signal detection, since inverse-scale rather than frequency is being used here. In addition, given its scaling covariance and localization properties, wavelet coefficients are considerably unaffected by localized noise in the data, which does not propagate to all coefficients as is the case with Fourier methods.

2. OBSERVATIONAL DATA

The photometric data used here make up an interrupted time series with a relatively poor signal-to-noise ratio and large intervals of daytime observational gaps. They were obtained in the 1 m telescope at the Sutherland site of the South African Astronomical Observatory. These observations were part of the largest spectroscopic and photometric campaign (to date) on PG 1605+072, using the Multi Site Spectroscopic Telescope (MSST). Several telescopes around the world were coordinated in aim to produce a long, high-quality continuous time series of that star's luminosity (Heber et al. 2003). The standard analysis of these photometric observations were made using Period98.[5] A full discussion of this work can be found in Pereira & Lopes (2004).

To prepare photometric observational data for time-frequency analysis, the data were resampled, or rebinned, and the daytime gaps and sampling observational irregularities were zero-padded.

[1] Centro de Física Teórica e Computacional, Complexo Interdisciplinar da Universidade de Lisboa, Avenida Prof. Gama Pinto, 2, 1649-003 Lisbon, Portugal; pmjorge@lip.pt.

[2] CENTRA, Departmento de Física, Instituto Superior Técnico, Avenida Rovisco Pais, 1049-001 Lisbon, Portugal; amaro@fisica.ist.utl.pt.

[3] Centro de Geofísica de Évora, Departamento de Física, Universidade de Évora, Colégio António Luis Verney, 7002-554 Évora, Portugal.

[4] Department of Physics, Denys Wilkinson Building, Keble Road, Oxford University, Oxford OX1 3RH, UK; lopes@astro.ox.ac.uk.

[5] See http://www.univie.ac.at/tops/Period04/index.html.

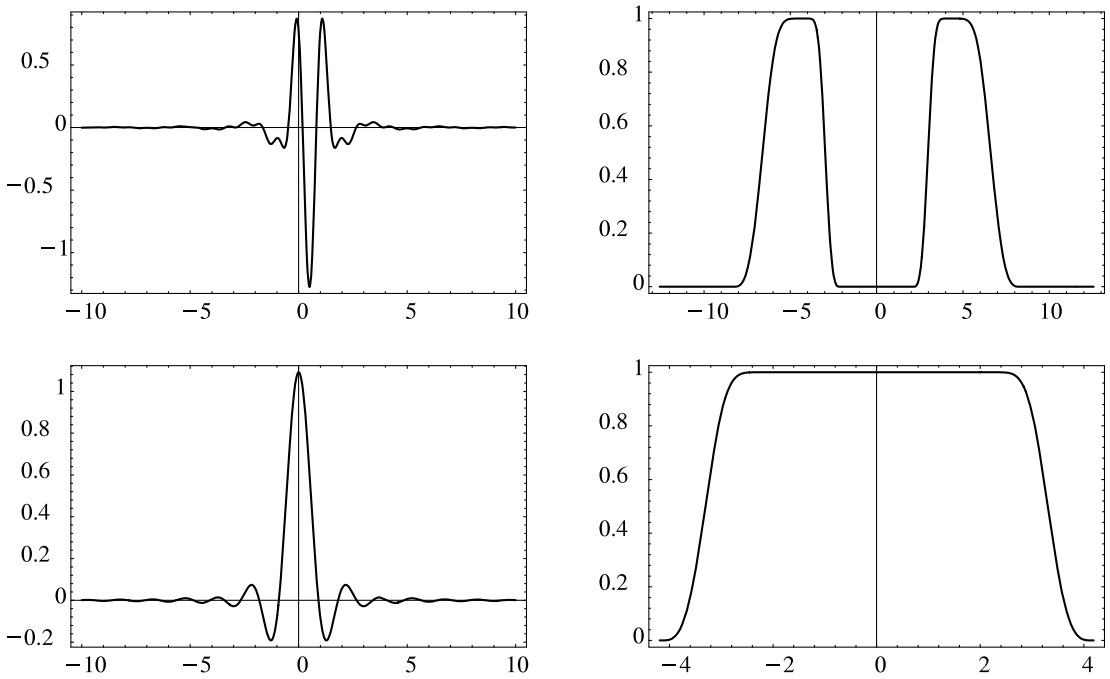

FIG. 1.—Meyer mother wavelet and its associated scaling function and filter functions. *Top left:* Wavelet function $\psi(t)$; *top right:* bandpass filter $\hat{\psi}(\omega)$; *bottom left:* scaling function $\phi(t)$; *bottom right:* low-pass filter $\hat{\phi}(\omega)$.

Furthermore, the beginning and end of the time series were also zeroed in order to obtain a sequence of 2^n elements. Both discrete local transforms were computed from this observational time series of 2^{16} elements.

3. LOCALIZED TIME-FREQUENCY ANALYSIS

The methods usually employed for "localizing" a time-frequency analysis may be characterized by the nature of the subdivision made to the time-frequency plane.

Local sine packet transforms (LSPTs) break the time axis of the time-frequency phase space in segments of different widths. In each of these time intervals, the frequency window size is fixed by the time duration of the segment. And two adjacent time windows of different sizes have frequency segmentation of different heights (see Fig. 2 below).

LSPTs, also referred to as Gabor transformations, provide windowed transformations that can adapt to the needs of different segments of a time series. This is a type of analysis that is well suited for a spectrum that shows peaks with spreads that are essentially not $1/T$ in nature. Gabor analysis is similar to a variable-window Fourier analysis that is adapted to different segments of the data. It can be complemented by methods that determine optimal segmentation of data and the corresponding choice of basis that is conducive to the smallest number of significant coefficients. This is one of the methods that we used to analyze the observational time series.

On the other hand, wavelet packet transform (WPT) is a multiresolution analysis that breaks the time-frequency plane in scale segments of different heights (scale $\sim$1/frequency). Scale divisions of different sizes bring time segmentation of different widths, so there is a more uniform treatment of oscillations during all observational time (see Fig. 3 below).

The set of bases is fixed when we choose the bell function in LSPT and the mother wavelet in WPT. In both cases, once we have chosen the basis generators, we can construct a binary tree of information of a signal by translations and dilations of those basis functions. The tree is built on the successive application of the appropriate decomposition to the previous blocks on the tree. Each level is a complete representation of the signal that covers all the time-frequency (or time-scale) plane allowed by the sampling. On one level of the tree all localization windows are equal. But other covers of the time-frequency plane exist that use information of different levels, thus bringing windows of different sizes.

Both methods may implement a best-basis search on the tree (Coifman & Wickerhauser 1991, 1992), where a choice of basis is done at different scales and locations according to some minimum criterion, thus providing the most economical and efficient representations of the signal with the chosen family of functions. This could conceivably be used for "spectral fingerprinting."

In this paper we use local sine packets with a polynomial bell function and Meyer wavelets (see Fig. 1), respectively, to generate the LSPT and WPT and their best basis relative to the signal at hand (see Figs. 2 and 3). We should mention that there are many levels of sophistication already developed for these techniques.

Using LSPT, we can improve the bell functions for better frequency localization, or take unequal intervals to construct the tree (Auscher et al. 1992; Wickerhauser 1991). In WPT, for instance, one can look for the best choice of wavelet family that optimizes the frequency localization capability of the respective wavelet packets (Coifman et al. 1992). Or one can generalize the wavelet packet formalism to use different families in each decomposition step of the tree (Hess-Nielsen 1994; Hess-Nielsen & Wickerhauser 1996).

We have refrained from going into too much technical sophistication just to make the point that, despite the fact that ours is not the optimal wavelet choice for harmonic frequency detection, it still provides excellent results at much lower resolution. A subband with 2^{12} frequency windows is used, which is four orders of magnitude lower than the standard Fourier methods used, for example, in Pereira & Lopes (2004). The method also provides a much nicer spectrum and better control over artifices of incomplete data.

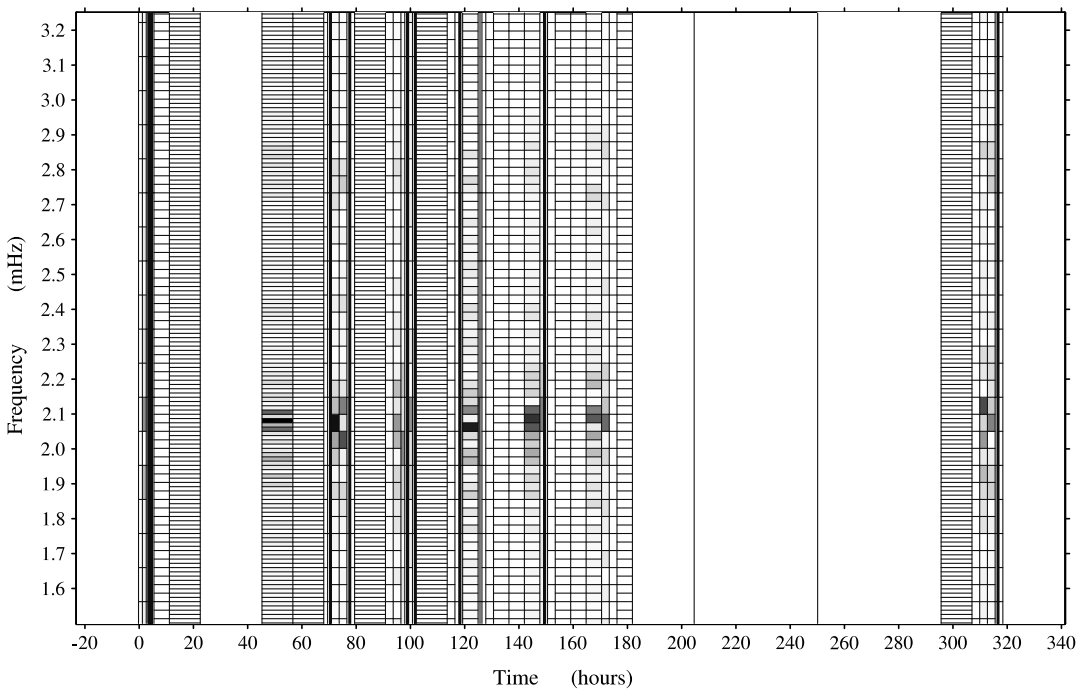

FIG. 2.—Time-frequency plane of the best-base representation of the signal with local sine packets. Gray values represent the relative importance of a local sine-packet contribution. White bands represent time windows (essentially daytime periods) for which the frequency subdivision is too tight to be usefully represented. Black means a higher absolute value of the coefficients. [*See the electronic edition of the Journal for a color version of this figure*.]

3.1. *Wavelet Package Transforms*

A wavelet frame $\{\psi_\alpha\}_{\alpha\in\mathcal{I}}$ is a collection of functions $\psi_\alpha(t)\in L^2_{\mathbb{R}}$ such that for any $f\in L^2_{\mathbb{R}}$, there are bounds $0<A\le B<\infty$ that verify

$$A\|f\|^2\le\sum_{\alpha\in\mathcal{I}}|\langle f,\ \psi_i\rangle|^2\le B\|f\|^2. \tag{1}$$

If $A=B=1$, then $\{\psi_\alpha\}_{\alpha\in\mathcal{I}}$ can be called a basis. If on the other hand $A=B>1$, redundancy exists and we call it a tight frame; i.e., an inversion formula exists anyway:

$$f(t)=A^{-1}\sum_{\alpha\in\mathcal{I}}\langle f,\ \psi_\alpha\rangle\psi_\alpha(t).$$

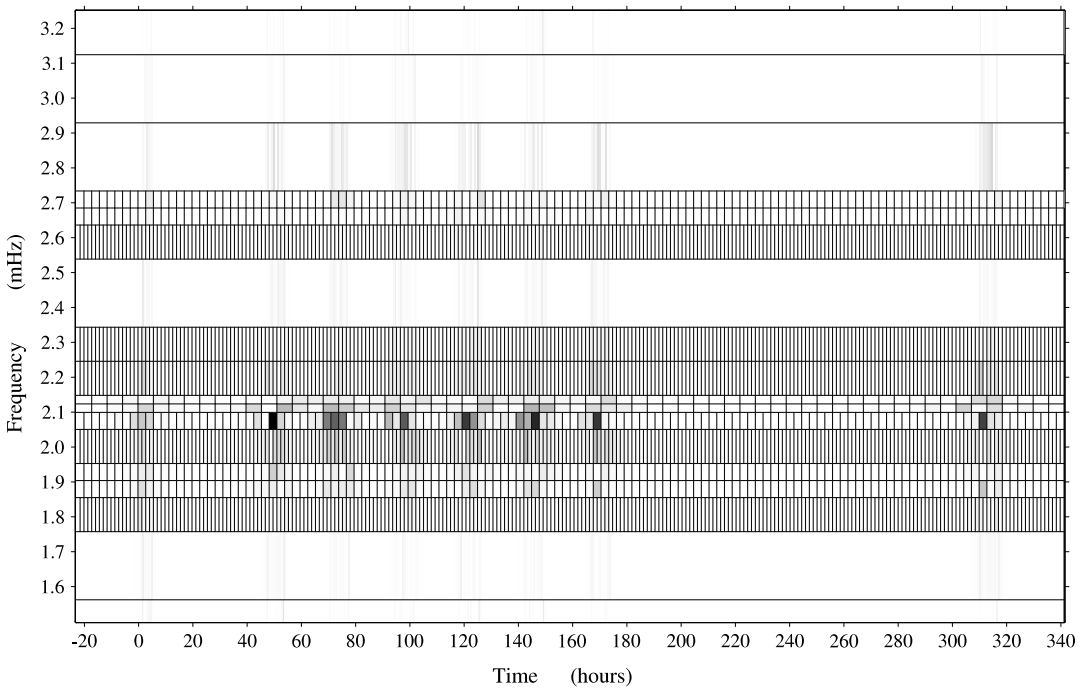

FIG. 3.—Time-frequency plane of the best-base representation of the signal with wavelet packets. Gray values represent the relative importance of a wavelet-packet contribution. White bands represent frequency windows at which the subdivision is too tight to be usefully represented. Black means a higher absolute value of the coefficients. [*See the electronic edition of the Journal for a color version of this figure*.]

Wavelet frames can be built from a single special function ψ, called the mother wavelet, by using flexible space-scale samplings (or, in this case, time-frequency samplings)

$$\psi_{ab}(t) = \frac{1}{\sqrt{a}}\psi\left(\frac{t-b}{a}\right). \tag{2}$$

Admissibility of ψ as a mother wavelet is conditioned by the inversibility condition, which essentially requires that

$$C_\psi = \int_{-\infty}^{+\infty} \frac{\left|\hat{\psi}(\omega)\right|^2}{|\omega|}\, d\omega < \infty. \tag{3}$$

The discrete wavelet transform (DWT) usually makes the dyadic choice $a = 2^{-j}$, $b = 2^{-j}k$ $(j,\ k \in \mathbb{Z})$ and corresponds then to a representation of the signal in terms of scaled and translated wavelets

$$\psi_{jk}(t) = 2^{j/2}\psi\left(2^j t - k\right). \tag{4}$$

For finite signals, this is a linear operation on a data vector of length 2^N, usually chosen to be invertible and orthogonal. A single level of a DWT will first generate 2^{N-1} coefficients $d_{N-1,k} = \langle f,\ \psi_{N-1,k}\rangle$ corresponding to details $\mathcal{D}_{N-1}$ at that scale. The remaining information needed to completely represent the signal can be chosen from an orthogonal subset of equal number of coefficients $s_{N-1,k} = \langle f,\ \phi_{N-1,k}\rangle$ corresponding to a smoothing $\mathcal{S}_{N-1}$ of the signal.[6] For the DWT this process is iterated on each smoothing component until we have the signal represented by mostly very small numbers (the wavelet coefficients corresponding to the details at different scales) and a few large numbers (basically the cumulative average). At each level, the scaling functions $\phi_{jk}(t)$ form a basis orthogonal to the $\psi_{jk}(t)$ and are in addition required to obey a dilation equation[7]

$$\phi_{N-1}(t) = \sum_k h_k \phi_{Nk}(t) = \sqrt{2}\sum_k h_k \phi_{N-1}(2t-k). \tag{5}$$

Equation (5) means that the space $\mathcal{S}_N$ (which is just our signal sampled to the maximum resolution 2^N) is in fact a direct sum $\mathcal{S}_N = \mathcal{D}_{N-1} \oplus \mathcal{S}_{N-1}$. But then the scaling functions ϕ_{Nk}, which form a basis for $\mathcal{S}_N$, besides generating $\mathcal{S}_{N-1}$ also generate any of the $\mathcal{D}_{N-1}$. The point is that we can determine coefficients $h_k,\ g_k$ for which this generation would look like equation (5) and[8]

$$\psi_{N-1}(t) = \sum_k g_k \phi_{Nk}(t) = \sqrt{2}\sum_k g_k \phi_{N-1}(2t-k). \tag{6}$$

[6] In this dyadic notation the mother wavelet corresponds to $\psi(t) = \psi_{N-1}(t)$ and the scaling function to $\phi(t) = \phi_{N-1}(t)$.

[7] This has to do with the way they are built on the Fourier-transformed space. The coefficients h_k, g_k (see eq. [6] below) are called filter coefficients, and they are the coefficients of the inverse Fourier transform of frequency response functions $H(\omega)$ and $G(\omega)$ that verify the scaling equations in Fourier space $\hat{\phi}(2\omega) = H(\omega)\hat{\phi}(\omega)$ and $\hat{\psi}(2\omega) = G(\omega)\hat{\phi}(\omega)$. These equations can be used to effectively build scaling and wavelet functions in Fourier space by iteration, as Meyer did.

[8] At each level j, the smoothing space $\mathcal{S}_j$ verifies $\mathcal{S}_j = \mathcal{D}_{j-1} \oplus \mathcal{S}_{j-1}$, and therefore we can represent both the scaling and the wavelet functions at level $j-1$ solely on the basis formed by the scaling functions ϕ_j at level j.

Generalizing this splitting concept to the details space, if we designate $\mathcal{W}_0(t) = \phi_{N-1}(t)$ and $\mathcal{W}_1(t) = \psi_{N-1}(t)$, then the set

$$\mathcal{W}_{2n}(t) = \sqrt{2}\sum_k h_k \mathcal{W}_n(2t-k), \tag{7}$$

$$\mathcal{W}_{2n+1}(t) = \sqrt{2}\sum_k g_k \mathcal{W}_n(2t-k) \tag{8}$$

generates a basis to decompose the detail spaces into direct sums $\mathcal{D}_j = \mathcal{D}_{j-1}^{\mathcal{D}_j} \oplus \mathcal{S}_{j-1}^{\mathcal{D}_j}$, as was done for $\mathcal{D}_{N-1}$ above, where we would have

$$\mathcal{W}_2(t) = \sqrt{2}\sum_k h_k \psi_{N-1}(2t-k), \tag{9}$$

$$\mathcal{W}_3(t) = \sqrt{2}\sum_k g_k \psi_{N-1}(2t-k). \tag{10}$$

The functions

$$\mathcal{W}_{mjk} = 2^{j/2}\mathcal{W}_m(2^j t - k) \tag{11}$$

are called wavelet packets, and a whole library of them exist into which a decomposition of the signal is possible. In this paper we have chosen to create a wavelet-packet basis from the Meyer ψ and ϕ functions (Fig. 1).

As we mentioned above, in DWT the variables j and k are integers that scale and translate the $\psi(t)$ to generate the wavelet frame. The scale index j indicates the wavelet's width, support, or variance (scale), and the location index k gives its mean position. The factor $2^{-j/2}$ is for the energy normalization across the different scales. Repeating the same operation for all possible j (in practice from $N = 2^j$ down, where N is the maximal resolution of our signal) yields a characteristic multiresolution analysis, based on dividing the signal at each level j into a smoothed part $\mathcal{S}_j$ and a details part $\mathcal{D}_j$ of equal size $n = 2^{j-1}$. At the next level, a simple wavelet transform would do the same for the smoothed part $\mathcal{S}_j$, leaving the details part $\mathcal{D}_j$ as it was. But a wavelet packet transform (WPT) can also change $\mathcal{D}_j$ instead, generating as a result new decimated smoothed and details parts. There are many ways we can do this (choosing at level j if we are going to use a transform of the $\mathcal{S}_j$ or $\mathcal{D}_j$ part), but there is a way to choose a best-basis decomposition to represent the signal, as we see in § 5.

3.2. *Localized Sine Packet Transforms*

An LSPT is essentially a variable windowed Fourier transform, as the frames are made of trigonometric functions multiplied by "soft" bell functions. By dilating and translating the bell functions that multiply the signal and then Fourier transforming it, we can have a complete representation of a signal.

LSPT follows closely from some of the proprieties of wavelet analysis, but it is complementary to the WPT in the sense that the LSPT gives priority to the time, while the WPT gives priority to the scales ($\sim$1/frequency). In a general LSPT we are choosing different time-window widths, and in each time interval the frequency-window heights are all equal. In the WPT we are choosing different frequency-window heights and in each scale interval all time-window widths are equal. But the areas of the cells are fixed, so that choosing width (height) fixes height (width). See Figures 2 and 3.

We consider bell functions that modulate a trigonometric function so that they behave as softened characteristic function in time. They go softly from zero to one and from one to zero.

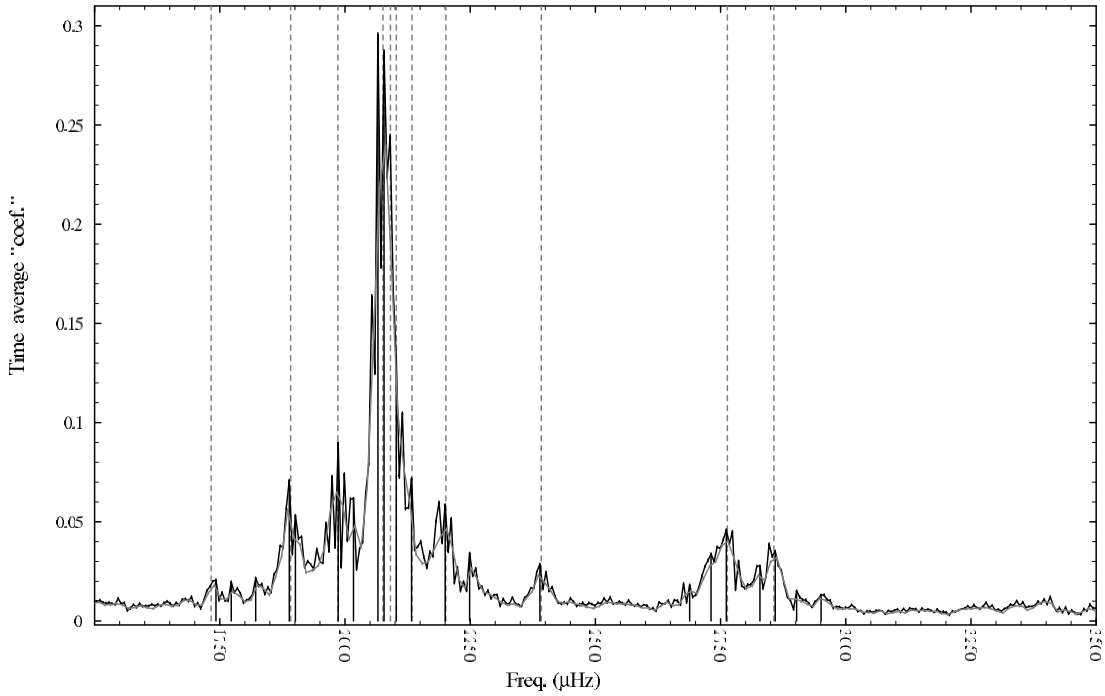

FIG. 4.—Amplitude spectrum for the seven-night combined data set: Time average of the wavelet packet transform coefficients at the 2^{11} (*gray*) and 2^{12} (*black*) subbands. Frequencies from Pereira & Lopes (2004) are shown as dashed vertical lines, WPT estimates as solid vertical lines. [*See the electronic edition of the Journal for a color version of this figure.*]

For the simplest construction,[9] let $\beta(t)$ be a continuous real-valued function on $\mathbb{R}$ that verifies

1. $\beta(t) = 0$ if $t < -1$;
2. $\beta(t) = 1$ if $t > 1$;
3. $\beta(t)^2 + \beta(-t)^2 = 1, \ \forall t$.

We are interested in functions β that are smooth on $]-1,\ 1[$ and have vanishing derivatives at the boundary, at least first-order ones.

Let us choose an equipartition of the real line with a sequence c_k, $k \in \mathbb{Z}$, so that $|c_k - c_{k-1}| =$ constant. Consider the intervals $L_k = [c_{k-1},\ c_{k+1}]$, which will be the support of our base, the middle point of the interval $[c_{k-1},\ c_k]$, $a_k = (1/2)(c_k + c_{k-1})$, and the half-length of it, $\lambda_l = (1/2)(c_k - c_{k-1})$. Since we took equally spaced $\{c_k\}$, $\{a_k\}$ will also be equally spaced, and we will have constant $|L_k|$ and $|I_k|$.

We can define a bell function with support in L_k by

$$b_k(t) = \begin{cases} \beta\left(\dfrac{t - a_k}{\lambda_k}\right), & \text{if } t \in [c_{k-1},\ c_k], \\ \beta\left(\dfrac{a_{k+1} - t}{\lambda_{k+1}}\right), & \text{if } t \in [c_k,\ c_{k+1}], \end{cases}$$

that localizes essentially in $I_k = [a_k,\ a_{k+1}]$.[10] "Injecting" frequencies in the bells, $\omega_{n,k}$, and renormalizing them to unity, we obtain an orthonormal basis of $L^2(\mathbb{R})$ made of the functions

$$g_{n,k}(t) = b_k(t)\sqrt{\frac{2}{|I_k|}}\sin\left[\omega_{n,k}\pi(t - a_k)\right]$$

for $n \in \mathbb{N}_0$ and $k \in \mathbb{Z}$, where

$$\omega_{n,k} = \frac{(n + 1/2)\pi}{|I_k|}.$$

The tails of adjacent basis functions overlap, but they are still made orthogonal functions by the choice of bells (see Auscher et al. 1992).

We can construct another subspace that localizes the signal essentially on $I_k \cup I_{k+1}$ generated by

$$B_k(t)\sqrt{\frac{2}{|I_k| + |I_{k+1}|}}\sin\left[\frac{(n + 1/2)\pi}{|I_k| + |I_{k+1}|}\pi(t - a_k)\right],$$

with $B_k^2(t) = b_k^2(t) + b_{k+1}^2(t)$, where the third constraint to the bell is useful. We get half as many time intervals and twice as many frequency intervals.[11]

This way, if we now consider a sampled signal of 2^N elements, we can repeat the process of binary joining the intervals until, in principle, we have one time interval and 2^N frequency windows, where the Fourier analysis is recovered. Actually we prefer to think of the splitting process. If we keep all the coefficients of the decomposition in each splitting step, we construct a binary library tree of all possible local sine basis representation. We used a polynomial bell.

4. FREQUENCY DETERMINATION

If we choose subbands of the binary-tree decomposition of any of these transforms we have a complete representation of

[9] A more general basis can be constructed for which the basis vectors are still localizing in time (mainly in $[a_k,\ a_{k+1}]$; see Auscher et al. 1992).

[10] Increased steepness of the sides of the bell yields better localization in frequency.

[11] Again, because $\{c_k\}$ were taken equally spaced, $|I_k|$ is constant and we get equally distant frequencies.

TABLE 1
Frequency Comparison

This Work LSPT 12 (μHz) (1)	This Work WPT 12 (μHz) (2)	PL 2004 (μHz) (3)	Kilk 1999 (μHz) (4)	O'Toole 2002 (μHz) (5)	Falter 2003 (μHz) (6)
1742	1742	1732.65	1744.40	...	...
1895	1889	1891.45	1891.42	1891.01	1891.4
1980	1986	1985.81	1985.32	1985.75	1985.8
2072	2078	2075.85	2075.76	2075.72	2075.9
2084	2090	2090.75	2085.84	...	...
2102	2102	2102.44	2103.28	2102.48	2102.0
2139	2133	2133.75	...	...	...
2200	2200	2201.49	2201.93	...	...
2389	2389	2391.90	2392.04	...	2392.0
2767	2761	2763.52	2761.30	2765.9	2763.7
2847	2847	2856.46	2846.47	...	...
4055	4061	4061.57	4061.81	...	4062.4
4147	4140	4140.68	4139.93	4151.48	...

Notes.—Comparison of this work's LSPT and WPT frequencies (± 3.1 μHz) with those of Pereira & Lopes (2004), Kilkenny et al. (1999), and O'Toole et al. (2002), and with the photometric UV_B study of Falter et al. (2003). Determined with 2^{13} resolution.

that signal that is a special packet transform. This corresponds to taking equal time-frequency boxes at high and low frequencies, as well as early and late times. In the LSPT case we recover the Gabor transform. With a signal of 2^{16} elements, any complete representation with these transforms must also have 2^{16} coefficients. In a subband if we have 2^h frequency boxes, we must have 2^{16-h} time boxes.

Figure 4 represents the time average of the WPT coefficients' modules, in order to compare it to the Fourier spectrum. It was from that averaged spectrum that we searched for the WPT frequencies in Table 1.

Taking a general LSPT with different boxes over time corresponds to considering different frequency boxes in each time interval, so the average over time would be incorrect. This is another reason for using this specific packet basis, besides keeping the same resolution at low and high frequencies. Moreover, when identifying "frequencies," we are interested in large time windows, which bring us shorter frequency windows and therefore better frequency resolution (see Fig. 5).

In Figure 6 we see that a subband containing 2^{12} frequency windows is quite accurate in pinpointing the spectrum profile. It is particularly accurate in identifying the maxima, even if at this

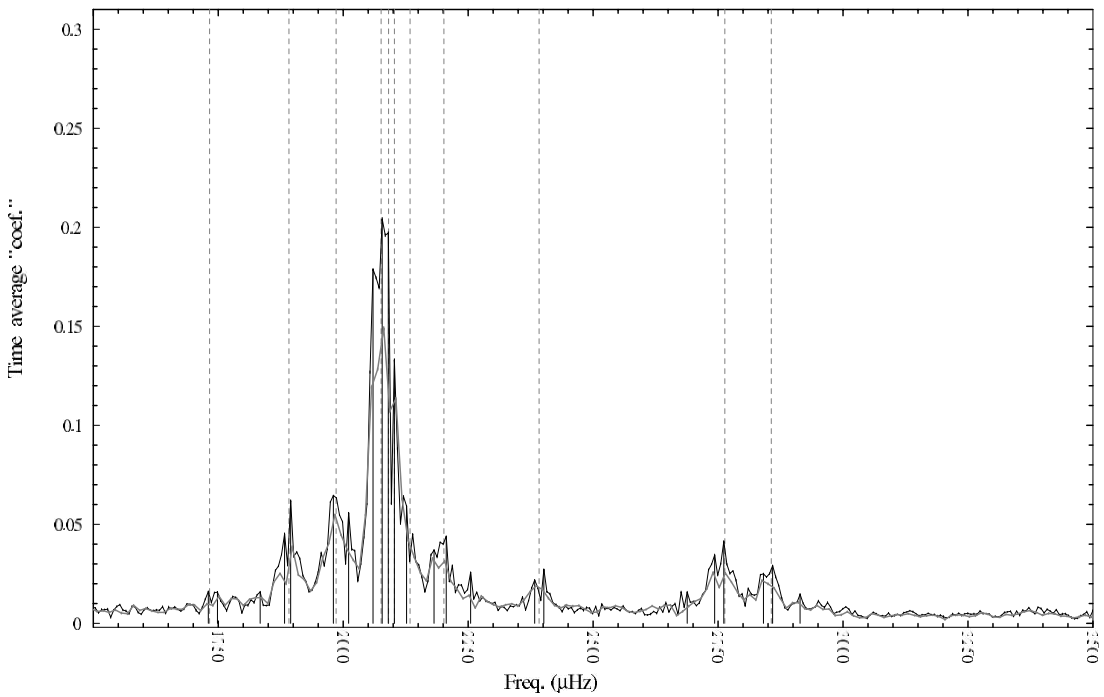

Fig. 5.—Amplitude spectrum for the seven-night combined data set: Time average of the local sine packet transform coefficients at the 2^{11} (*gray*) and 2^{12} (*black*) subbands. Frequencies from Pereira & Lopes (2004) are shown as dashed vertical lines and LSPT estimates as solid vertical lines. [*See the electronic edition of the Journal for a color version of this figure.*]

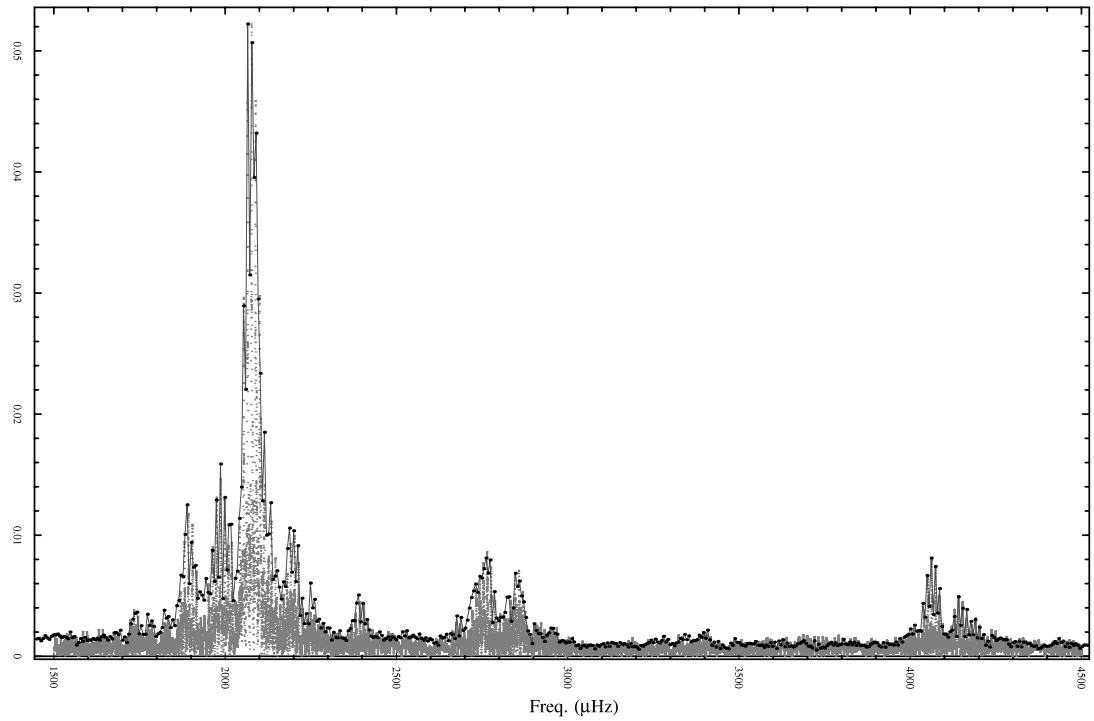

FIG. 6.—Amplitude spectrum for the seven-night combined data set: Observed pulsation spectrum of the star PG 1605+72 using a conventional Fourier transform (*gray*) and the WPT 2^{12} subband (*black dots*). The profile is enhanced by a black line joining the dots. [*See the electronic edition of the Journal for a color version of this figure*.]

resolution there is difficulty resolving some of the peaks composed of multiple frequencies. We also should mention that lower resolution in frequency spectra leads to an averaging effect and the corresponding smoothing of the spectra (see versions of WPT and LSPT at the 2^{11} subband in Figs. 4 and 5).

We could refine and go to higher frequency resolutions, but a compromise must be made, since frequency spreading in WPT and oscillation phenomena in LSPT show up as we approach maximum frequency resolution (Hess-Nielsen 1994).

5. BEST-BASIS SELECTION AND SIGNAL RECONSTRUCTION

The identification of the signal is a process of representation, be it by frequency, by amplitude and phase coefficients, or by wavelet packet coefficients. In addition to a good fit to the experimental data, a smaller number of coefficients is usually regarded as a property of a good representation. Compression is natural in the wavelet domain, since cancellation of some low-valued coefficients will tend to affect details only locally in the signal, whereas in the Fourier domain every coefficient has global effects. In order to minimize the number of coefficients needed to represent our data we use an entropy criterion developed by Coifman & Wickerhauser (1992) and Wickerhauser (1991). This corresponds to minimizing an "entropy function" $\mathcal{E}(\{w_J\})$ over the set of N coefficients w_J, where $J = mjk$, obtained by decomposing the signal $\mathcal{S}_N$ into each possible choice of wavelet-packet basis $\{\mathcal{W}_J\}$ for a particular mother wavelet $\psi(t)$ and corresponding scaling function $\phi(t)$. Defining a normalized probability distribution $p_J = w_J^2 / \sum_J w_J^2$ for each choice of basis, then the function

$$\mathcal{E}(\{\mathcal{W}_J\}) = -\sum_J p_J \log_2(p_J) \qquad (12)$$

should be a minimum for the best basis $\{\mathcal{W}_J\}$; i.e., the basis that needs the lowest number of components to effectively represent the signal. At this point it is debatable whether this is the best criterion for selection of a basis, when economy factors should give way to frequency precision goals. In this work we chose to look for the best basis associated with the Meyer wavelet and scaling functions. This choice of mother wavelet is probably not optimal for this signal, but we use it to illustrate that, as a tool for spectrum analysis, many choices of wavelet will give very good results (i.e., more economical and with better resolution at larger scales than Fourier approaches). As already mentioned by other authors (Coifman et al. 1992; Hess-Nielsen 1994; Hess-Nielsen & Wickerhauser 1996), there are proposals to investigate wavelets that would allow optimal determination of frequencies, which we chose not to follow in this paper.

In Figures 7–10 we reconstruct the observation data using Meyer's wavelet packet best basis for the signal (Fig. 3). We adopted several compression schemes, and the first (and most common) is to eliminate all WPT coefficients below a cutoff value. Figures 7 and 8 are examples of reconstruction of the third observation night, corresponding respectively to 98.33% and 99.88% compression. From these we see (Fig. 8) that higher compression degrades the reconstruction quality mostly at the end zone, where low-frequency contributions seem to dominate.

The last two figures (Figs. 9 and 10) reflect another compression scheme in which a restriction in the frequencies allowed for reconstruction is first imposed on the WPT of the signal, and then a cutoff is applied. The logic behind this is to isolate possible low-frequency noise from the main spectrum, a common measure when using Fourier reconstruction techniques. The cutoff value of 56×10^{-3} in the squares of WPT coefficients was determined to result in a reconstruction of the signal using the same amount of information as was used in Pereira & Lopes (2004); i.e., 39 coefficients in all (Fig. 10). The frequency

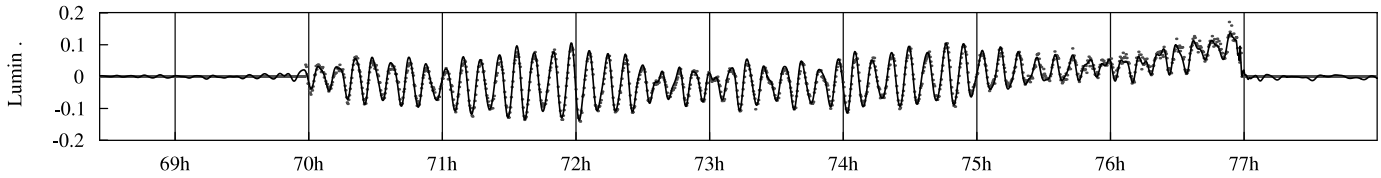

FIG. 7.—Reconstruction of the third night's data with simple compression (98.33%), using 1096 coefficients with squares larger than a cutoff of 10^{-3} in Meyer's WPT best basis (Fig. 3). [*See the electronic edition of the Journal for a color version of this figure*.]

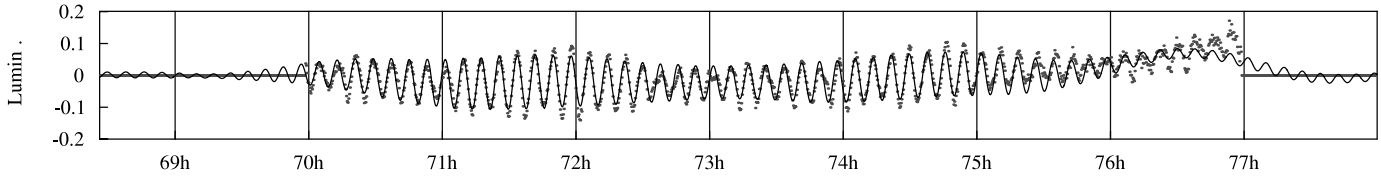

FIG. 8.—Reconstruction of the same data as above, but with a higher compression (99.88%), corresponding to the 78 coefficients above a cutoff of 56×10^{-3} in the same basis. [*See the electronic edition of the Journal for a color version of this figure*.]

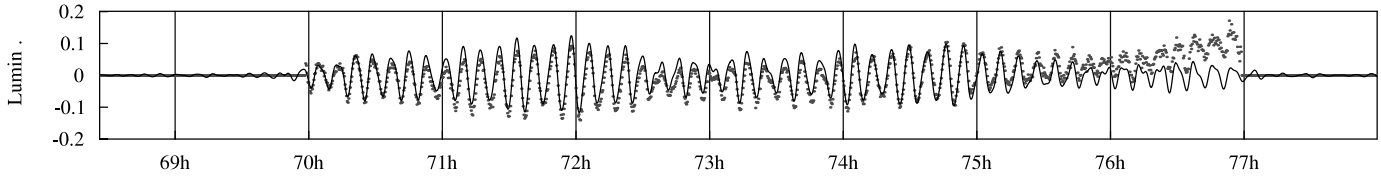

FIG. 9.—Using only frequencies from the spectrum shown in Fig. 6 (i.e., dropping low- and high-frequency components), we get a 99.06% compression with 614 coefficients above a cutoff of 10^{-3}. [*See the electronic edition of the Journal for a color version of this figure*.]

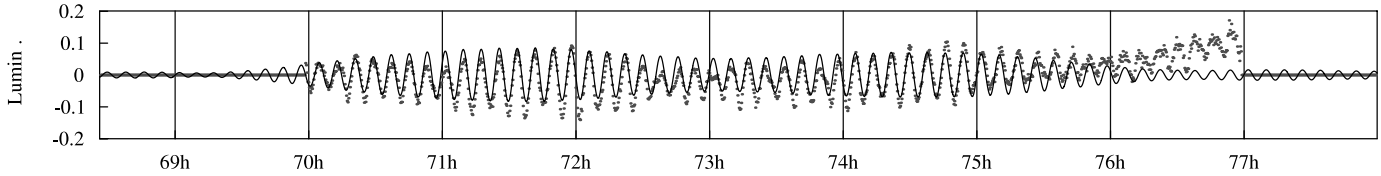

FIG. 10.—Again, dropping low-frequency components and using as few as 39 coefficients above a cutoff of 56×10^{-3} (the same amount of information as used in the Fourier fit in Pereira & Lopes 2004), we obtain a reconstruction with 99.94% compression. [*See the electronic edition of the Journal for a color version of this figure*.]

bandwidth was also the same as in the cited reference, and it is included in the range shown in Figure 6. The other cutoff at 10^{-3} in WPT space yields a better reconstruction with 614 coefficients (99.06% compression; see Fig. 9) but is still much worse than that of Figure 7, where the same cutoff was used on all frequencies.

As we can see in these images, low frequencies are essential to a good reconstruction. Suppressing them shows that some noise does occur at the end of the observation period each night, but there are also genuine star luminosity periodicities in that low-frequency band, because the signal dies away faster than expected as compared to the remainder of the signal. Further work should be done on separation and detection of true low-frequency contributions and identification of the low-frequency noise.

6. CONCLUSION

Time-frequency analysis has been used by many people in many different fields of research. Nevertheless, this type of analysis is far from being the mainstream data research toolbox. Wavelet techniques are a tool that expands the Fourier analysis with so many advantages that we believe its use should be widespread (Chui 1992; Daubechies 1992; Hess-Nielsen & Wickerhauser 1996).

While we do not propose to comprehensively study those advantages in this work, we apply the aforementioned techniques to do a time-frequency analysis of a signal measured over some nights for which the diurnal information is absent. This is a classical study in which Fourier analysis is the standard procedure, with some well-known problems that are overcome by the analysis proposed in this work.

In this paper we studied the pulsating spectrum of sdB PG 1605+072. Subdwarf B stars are known to present nonlinear stellar pulsations, namely, in the upper layers of the star where the pulsation are strongly nonadiabatic; this fact is well established once the timescale of stellar pulsation is of the same order of magnitude of the transport of energy in the outer layers of the star. Therefore, a general technique such as the wavelet analysis allows a better determination of periodicities of the pulsation spectrum. In fact, the representation of stellar pulsations as a series of harmonic functions is actually a strong simplification of the observed pulsations on these stars.

By looking for luminosity variations in the PG 1605+072 photometry data, we essentially confirm, by an independent method, the frequencies of the modes of vibration already studied by Pereira & Lopes (2004), Kilkenny et al. (1999), O'Toole et al. (2002), and Falter et al. (2003). A careful analysis of Table 1 and Figures 4–5 highlights the accuracy of the proposed methods discussed in this paper, and in particular of the WPT method. The LSPT method (col. [1]) shows the ability to identify the same frequencies as the classical Fourier analysis, nevertheless has a lower consistency with those determined in previous campaigns. An excellent agreement is found between the WPT method (col. [2]) and the results obtained by previous observational campaigns, namely, the campaign from Kilkenny et al. (1999), which has time series of 180 hr over five observational sites (col. [4]). The results obtained with WPT methods seem quite interesting, if we recall that our analysis is done on a observational time series of 45 hr, obtained on a single site during 15 nights.

Furthermore, this type of analysis introduces a new concept of periodicity that is related to the inverse timescale, rather than the harmonic frequency concept basic to Fourier. This means that deformations and instantaneous perturbations of the harmonic components will not affect the spectra in a global manner, thus yielding a more robust means of periodicity determination. Of course some of the frequencies detected might belong to an altogether nonharmonic event, in which case new physics might be present.

The best-base criterion for representation of both packet transforms was shown to be not only economical, but provided also some insight into the main spectral contributions of the signal. It was used to create a scheme of band-suppressed compression and to illustrate the differences in LSPT and WPT representations, displaying the dual windowing schemes that are invoked when analyzing and/or reconstructing the signal.

In summary, the results presented in this paper strongly suggest that wavelet packet basis analysis of stellar pulsation time series can be an excellent methodology to obtain the pulsation frequencies and other periodicities from observed light curves. Furthermore, in general, methods of wavelet analysis may shed new light on the spectrum of pulsation stars and improve the diagnostic tools of observational asteroseismology.

REFERENCES

Auscher, P., Weiss, G. L., & Wickerhauser, M. V. 1992, in Wavelets: A Tutorial in Theory and Applications, ed. C. K. Chui (San Diego: Academic Press), 237

Chui, C. K. 1992, An Introduction to Wavelets (San Diego: Academic Press)

Coifman, R. R., Meyer, Y., & Wickerhauser, M. V. 1992, in Wavelets and Their Applications, ed. M. B. Ruskai et al. (Boston: Jones and Bartlett), 453

Coifman, R. R., & Wickerhauser, M. V. 1992, IEEE Trans. Inf. Theory, 32, 712

Daubechies, I. 1992, Ten Lectures on Wavelets (Philadelphia: SIAM)

Falter, S., Heber, U., Dreizler, S., Schuh, S. L., Cordes, O., & Edelmann, H. 2003, A&A, 401, 289

Goupil, M., Auvergne, M., & Baglin, A. 1991, A&A, 250, 89

Heber, U., et al. 2003, in White Dwarfs, ed. D. de Martino et al. (Dordrecht: Kluwer), 105

Hess-Nielsen, N. 1994, Appl. Comput. Harmonic Analysis, 1, 157

Hess-Nielsen, N., & Wickerhauser, M. V. 1996, Proc. IEEE, 84, 523

Kilkenny, D., et al. 1999, MNRAS, 303, 525

Koen, C., O'Donoghue, D., Kilkenny, D., Lynas-Gray, A. E., Marang, F., & van Wyk, F. 1998, MNRAS, 296, 317

O'Toole, S. J., Bedding, T. R., Kjeldsen, H., Dall, T. H., & Stello, D. 2002, MNRAS, 334, 471

Pereira, T. M. D., & Lopes, I. P. 2004, A&A, 426, 213

———. 2005, ApJ, 622, 1068

Serre, B., Roques, S., Pfeiffer, B., Dolez, N., Vauclair, G., Maréchal, P., & Lannes, A. 1995, in Proc. 9th European Workshop on White Dwarfs, ed. D. Koester & K. Werner (Berlin: Springer), 299

Vigouroux, A., & Delache, P. 1993, A&A, 278, 607

Wickerhauser, M. V. 1991, in Problémes Non-Linéaires Appliqués, Ondelettes et Paquets D'Ondes, ed. P.-L. Lions (Roquencourt: INRIA), 31

Woolf, V. M., Jeffery, C. S., & Pollacco, D. L. 2002, MNRAS, 329, 497